

## Properties of the D Mesons\*

G.J. Feldman

Stanford Linear Accelerator Center  
Stanford University, Stanford, California

### I. Introduction

The purpose of this talk is to review what we have learned from the study of non-leptonic decays of D mesons.<sup>1</sup> The relevant world data come from two experiments which were performed using the same detector, the SLAC-LBL magnetic detector at SPEAR.<sup>2</sup> SLAC experiment SP17 ran on the magnetic detector through July 1976; experiment SP26 ran from October 1976 through June 1977. The SP17 data which we shall use are published<sup>3</sup> or have been submitted for publication.<sup>4,5</sup> However, with one exception,<sup>6</sup> the SP26 data are unpublished and preliminary.<sup>7</sup>

In section II, we shall review briefly the measurements of the  $\psi(3772)$  since it will play a major role in the determination of D meson properties. Section III will discuss the accurate determination of D masses and their consequences. Inclusive measurements and tagged events will be the subjects of sections IV and V, respectively. The distinction between inclusive measurements and tagged events is that in the former one detects a D decay and ignores the remainder of the event, while in the latter, one detects a D decay and studies the remainder of the event.

Due to a lack of time, we shall not be able to cover a number of important topics on which we have experimental information. These include D and D\* spins,<sup>8</sup>  $D^0$ - $\overline{D}^0$  mixing,<sup>3,4</sup> and  $\rho$  and K\* formation in D decays.<sup>5,9</sup>

---

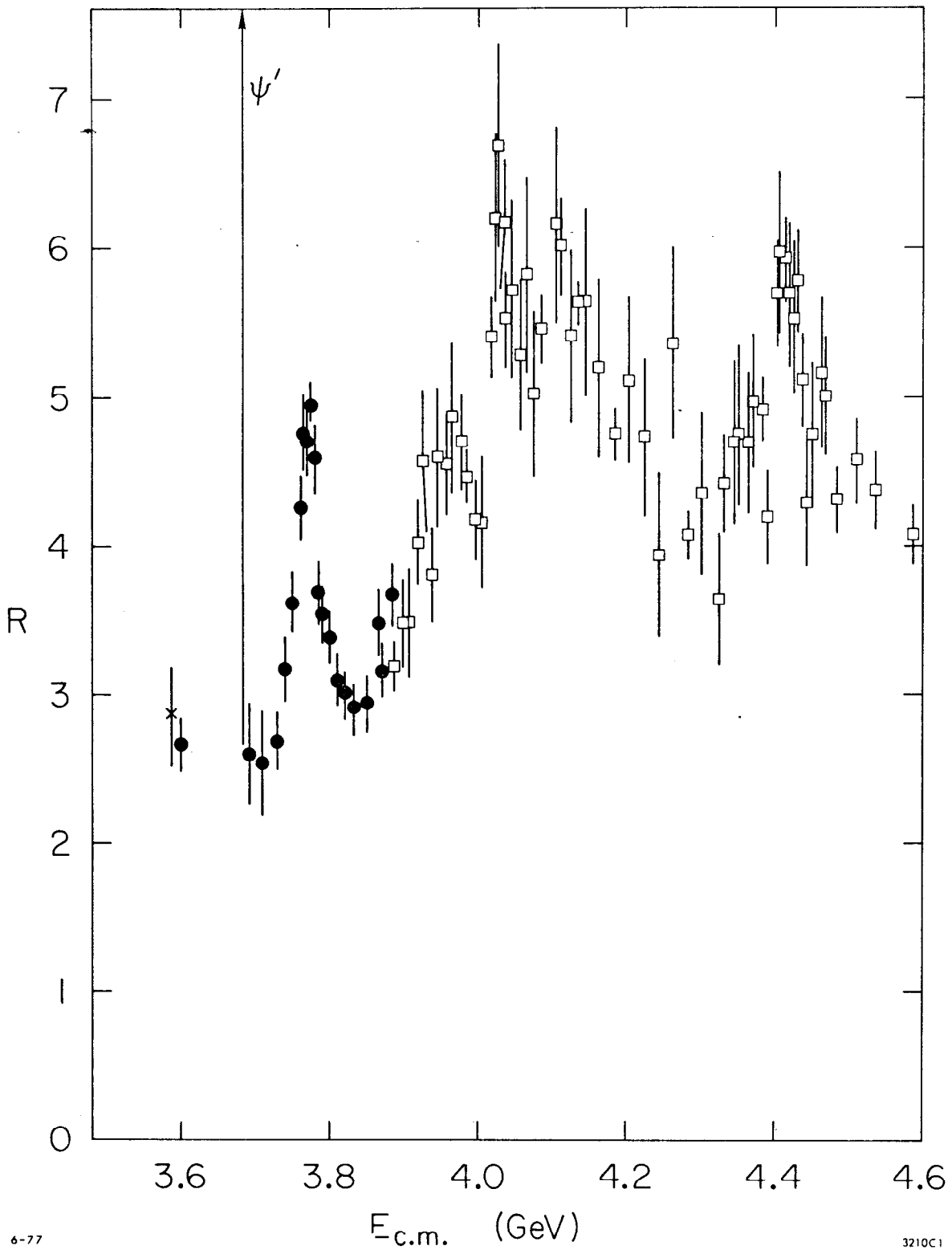
\*Work supported by the Energy Research and Development Administration.  
(Invited talk at the SLAC Summer Institute on Particle Physics, July 11-22, 1977, Stanford, California.)

## II. $\psi(3772)$

Figure 1 shows the ratio R of the total cross section for hadron production to the cross section for the production of  $\mu$  pairs in the energy region 3.6 to 4.6 GeV. The closed circles represent recent SP26 data<sup>6</sup> and show a clear resonance near 3.77 GeV, just above the threshold for the production of D meson pairs. The crossed point<sup>10</sup> and the open squares<sup>11</sup> represent older SP17 data. It is interesting to note that there are sharp rises in R just after each of the D and D\* thresholds:  $D\bar{D}$  at 3.727 GeV,  $D\bar{D}^*$  at 3.869 GeV, and  $D^*\bar{D}^*$  at 4.012 GeV.

The question most often asked upon showing someone Figure 1 is "How was it missed before?" The answer is twofold. First, Figure 1 has been corrected for radiative effects in the initial state. The data before these corrections are shown in Fig. 2a, and these data correspond to what we actually observe. The  $\psi(3772)$  (or  $\psi''$ ) is partially obscured by the  $\psi'$  radiative tail, and is thus harder to see in a cross section scan. The second part of the answer is simply that insufficient data were collected in this energy region. Evidence for the  $\psi''$  at the two standard deviation level was actually obtained over a year ago.<sup>12</sup>

The next most often asked question is "Into what does it decay?" A partial answer is provided by Fig. 3 which shows the cross section times branching fraction ( $\sigma \cdot B$ ) for the D decay into  $K^{\mp} \pi^{\pm}$ . It is clear that  $D\bar{D}$  is one of the resonant channels. Through section IV we will assume that  $D\bar{D}$  is the only substantial decay mode of the  $\psi''$ . The rationale is that the  $\psi'$  and  $\psi''$  differ in mass by only  $88 \text{ MeV}/c^2$  and thus should have similar decay modes to channels which are open to both states. However, the total  $\psi''$  width is two orders of magnitude larger than the  $\psi'$  width. The simplest explanation for the difference in widths is to



6-77

3210C1

FIG. 1.  $R$  vs.  $E_{c.m.}$

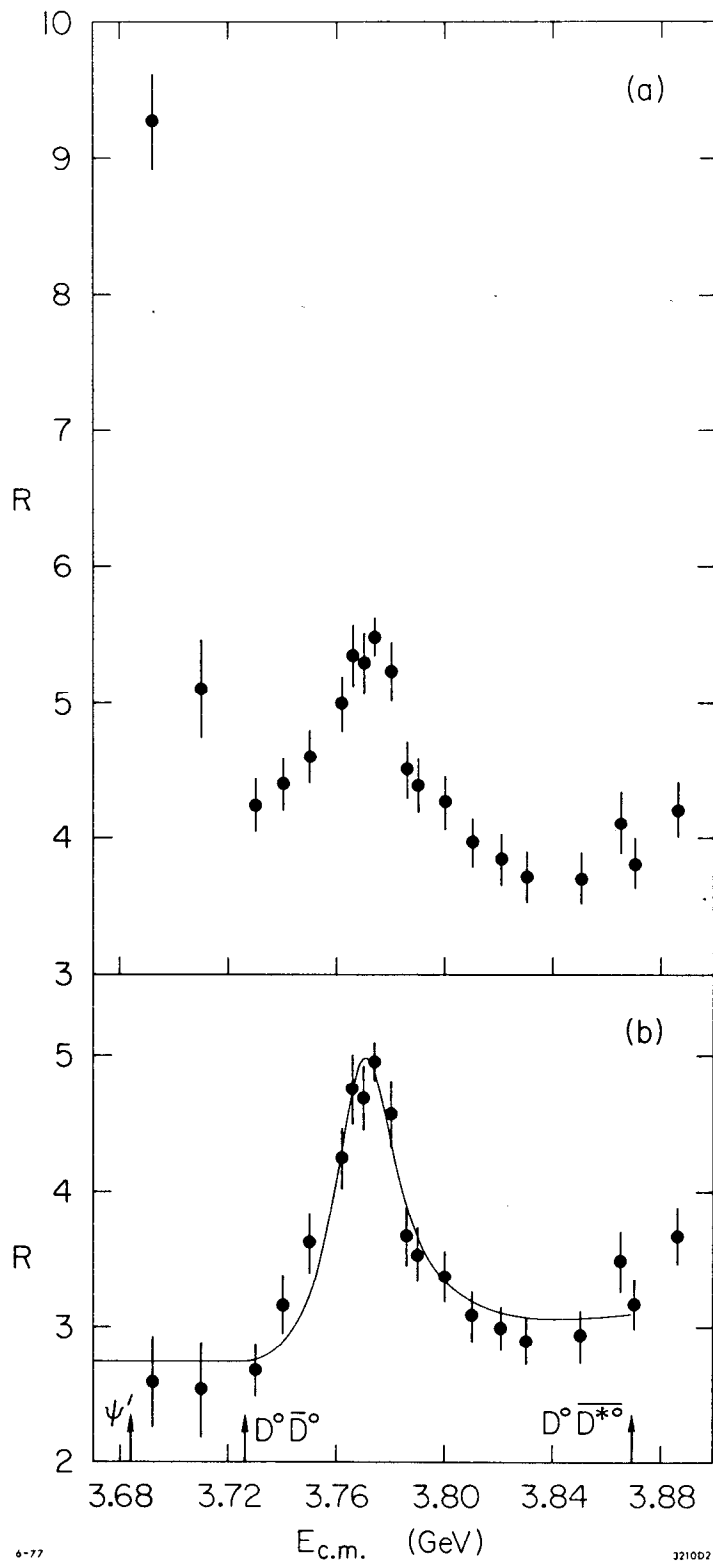


FIG. 2.  $R$  vs.  $E_{c.m.}$  (a) before and (b) after corrections for radiative effects. The curve is a p-wave Breit-Wigner shape described in the text.

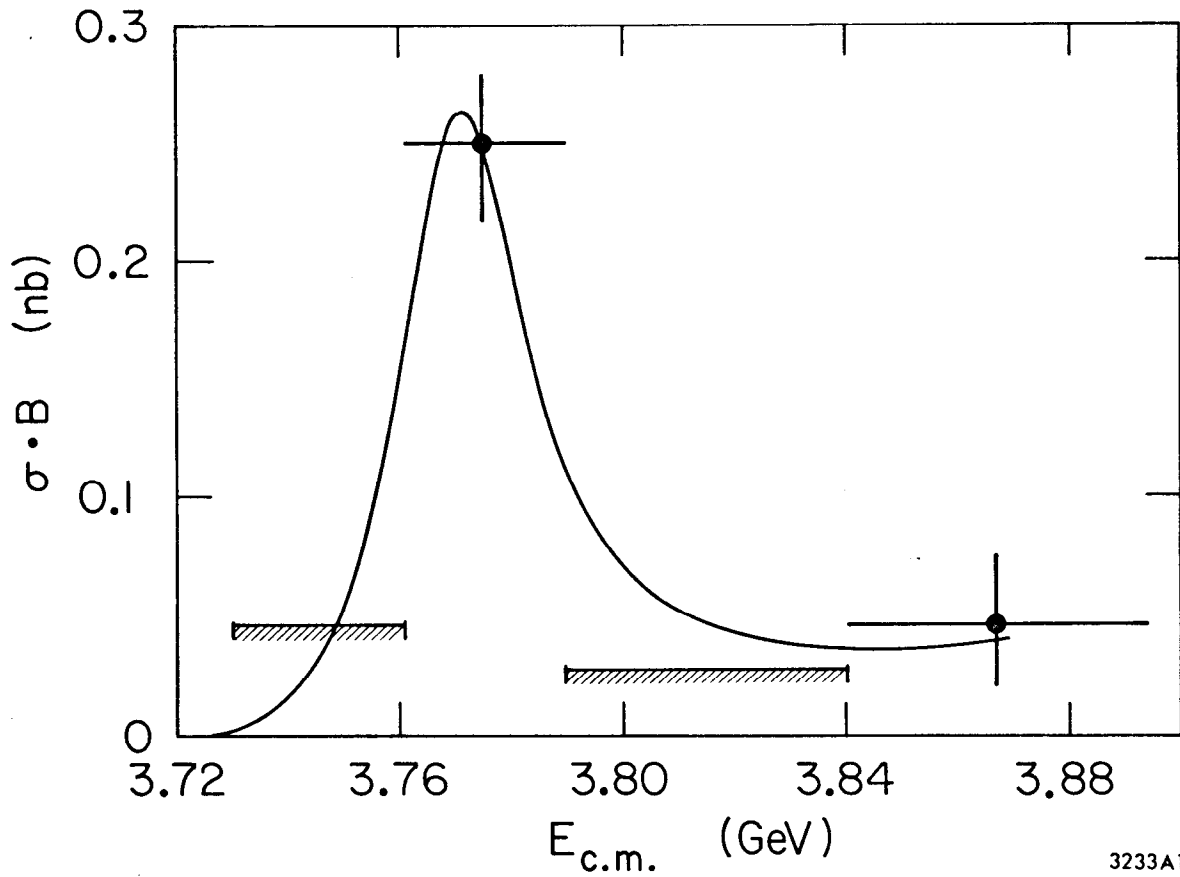


FIG. 3.  $\sigma \cdot B$  for  $D^0 \rightarrow K^\mp \pi^\pm$  vs.  $E_{c.m.}$ . The curve is the  $\psi'$  line shape and charmed particle background parameterization shown in Fig. 2.

attribute most of the  $\psi''$  width to the  $D\bar{D}$  channel, which is accessible to it, but not to the  $\psi'$ . This is a dramatic example of the Okubo-Zweig-Iizuka rule. In section V, we will show that the measured  $\psi'' \rightarrow D\bar{D}$  branching fraction is consistent with this assumption.

To fit the  $\psi''$  line shape we use the Breit-Wigner form

$$R = \frac{3\pi}{\sigma_{\mu\mu} m^2} \frac{\Gamma_{ee} \Gamma(E)}{(E_{c.m.} - m)^2 + \Gamma^2(E)/4} \quad (1)$$

To account for the proximity of the  $D\bar{D}$  threshold, we give the width  $\Gamma$  an energy dependence

$$\Gamma(E) \propto \frac{p_0^3}{1 + (rp_0)^2} + \frac{p_+^3}{1 + (rp_+)^2}, \quad (2)$$

where  $p_0$  and  $p_+$  represent the momenta of a  $D^0$  and a  $D^+$  respectively, from  $D$  pair production, and  $r$  represents an interaction radius.<sup>13</sup> In writing Eq. 2 we have assumed that, except for phase space, decays to  $D^0\bar{D}^0$  and  $D^+D^-$  are equally likely. This is equivalent to assuming that the  $\psi''$  has a definite isospin, either 0 or 1. Although this assumption is not crucial here, it will become important in section IV.

We have obtained acceptable fits for all values of  $r$  greater than 1 fm. Figure 2b shows a fit for  $r = 3$  fm. It is interesting to note that fits with energy independent widths give considerably better  $\chi^2$ 's than the one shown in Fig. 2b. This is due to the inability of the p-wave fits to accommodate the high values of  $R$  on the leading edge. This effect is not significant in the present data, but warrants watching.

The results of the fits to the  $\psi''$  and the other isolated  $\psi$  resonances are given in Table I.<sup>6,11,14,15</sup> This Table differs from the original papers in not including the 0.13% uncertainty in the absolute SPEAR energy calibration.

Thus the  $\psi$  is defined to have mass  $3095 \text{ MeV}/c^2$  and all other mass measurements are technically measurements of the ratio of a given mass to the  $\psi$  mass. This convention is necessary to give meaning to the D mass measurements which will be presented in the next section and which have a precision of better than one part in  $10^3$ .

TABLE I

Resonance parameters for the isolated  $\psi$  resonances.  $\Gamma$  is the full width,  $\Gamma_{ee}$  is the partial width to electron pairs, and  $B_{ee}$  is the branching fraction to electron pairs. See the text for an explanation of the errors on the mass.

State	Mass ( $\text{MeV}/c^2$ )	$\Gamma$ ( $\text{MeV}/c^2$ )	$\Gamma_{ee}$ ( $\text{keV}/c^2$ )	$B_{ee}$
$\psi$	3095	$0.069 \pm 0.015$	$4.8 \pm 0.6$	$0.0069 \pm 0.009$
$\psi'$	$3684 \pm 1$	$0.228 \pm 0.056$	$2.1 \pm 0.3$	$(9.3 \pm 1.6) \times 10^{-3}$
$\psi''$	$3772 \pm 3$	$28 \pm 5$	$0.37 \pm 0.09$	$(1.3 \pm 0.2) \times 10^{-5}$
$\psi(4414)$	$4414 \pm 5$	$33 \pm 10$	$0.44 \pm 0.14$	$(1.3 \pm 0.3) \times 10^{-5}$

### III. Masses

#### A. $D^0$ and $D^+$ Masses

To calculate a mass one uses the formula

$$m = (E^2 - p^2)^{1/2} . \quad (3)$$

The advantage of studying  $e^+e^- \rightarrow D\bar{D}$  is that the energy  $E$  must equal  $E_b$ , the energy of one of the incident beams.  $E_b$  has an rms spread, due to quantum fluctuations in synchrotron radiation, of only about 1 MeV,<sup>16</sup> and its central value can be monitored to high precision.<sup>17</sup> For  $D\bar{D}$  production near threshold, as in  $\psi''$  decays, we have the additional advantage that

$p^2$  is small, about  $0.08 \text{ (GeV/c)}^2$ . Thus any error in  $p$  is demagnified in its effect on the determination of the mass. The final result is that we measure masses in  $\psi'$  decays with an rms resolution of about  $3 \text{ MeV/c}^2$ , which is a factor of 5 to 10 better than they can be measured at higher energies.

Charged kaons are identified by time-of-flight measurements<sup>18</sup> and neutral kaons are identified by measurement of the dipion mass and the consistency of the dipion vertex with the assumed kaon decay.<sup>19</sup> For each particle combination we first require that the measured energy agree with  $E_b$  to within 50 MeV and then calculate the mass from Eq. 3 with  $E = E_b$ . The results, given in Fig. 4 in  $4 \text{ MeV/c}^2$  wide bins, show clear signals in five modes including the previously unreported mode  $D^+ \rightarrow K_S^+ \pi^+$ . Figure 5 shows the  $D^+$  and  $D^0$  mass spectra for the sum of all observed modes in  $2 \text{ MeV/c}^2$  bins. The mass difference of about  $5 \text{ MeV/c}^2$  between the  $D^+$  and  $D^0$  is clearly visible. Fits to the mass spectra give

$$M_{D^0} = 1863.3 \pm 0.9 \text{ MeV/c}^2 \quad (4)$$

and

$$M_{D^+} = 1868.4 \pm 0.9 \text{ MeV/c}^2 \quad (5)$$

The errors are dominated by systematic uncertainties such as the absolute momentum calibration and the stability of  $E_b$  monitoring. The  $D^+ - D^0$  mass difference is determined to be  $5.1 \pm 0.8 \text{ MeV/c}^2$ ; it is known more precisely than either  $D$  mass because several systematic errors cancel in the mass difference. The theoretical estimate of this mass difference has been widely discussed with estimates ranging from 2 to  $15 \text{ MeV/c}^2$ .<sup>20</sup>

### B. $D^{*0}$ Mass

To obtain the  $D^{*0}$  mass we employ the same trick with  $D^{*0} \overline{D^{*0}}$  production at 4.028 GeV with the following differences:<sup>4</sup>

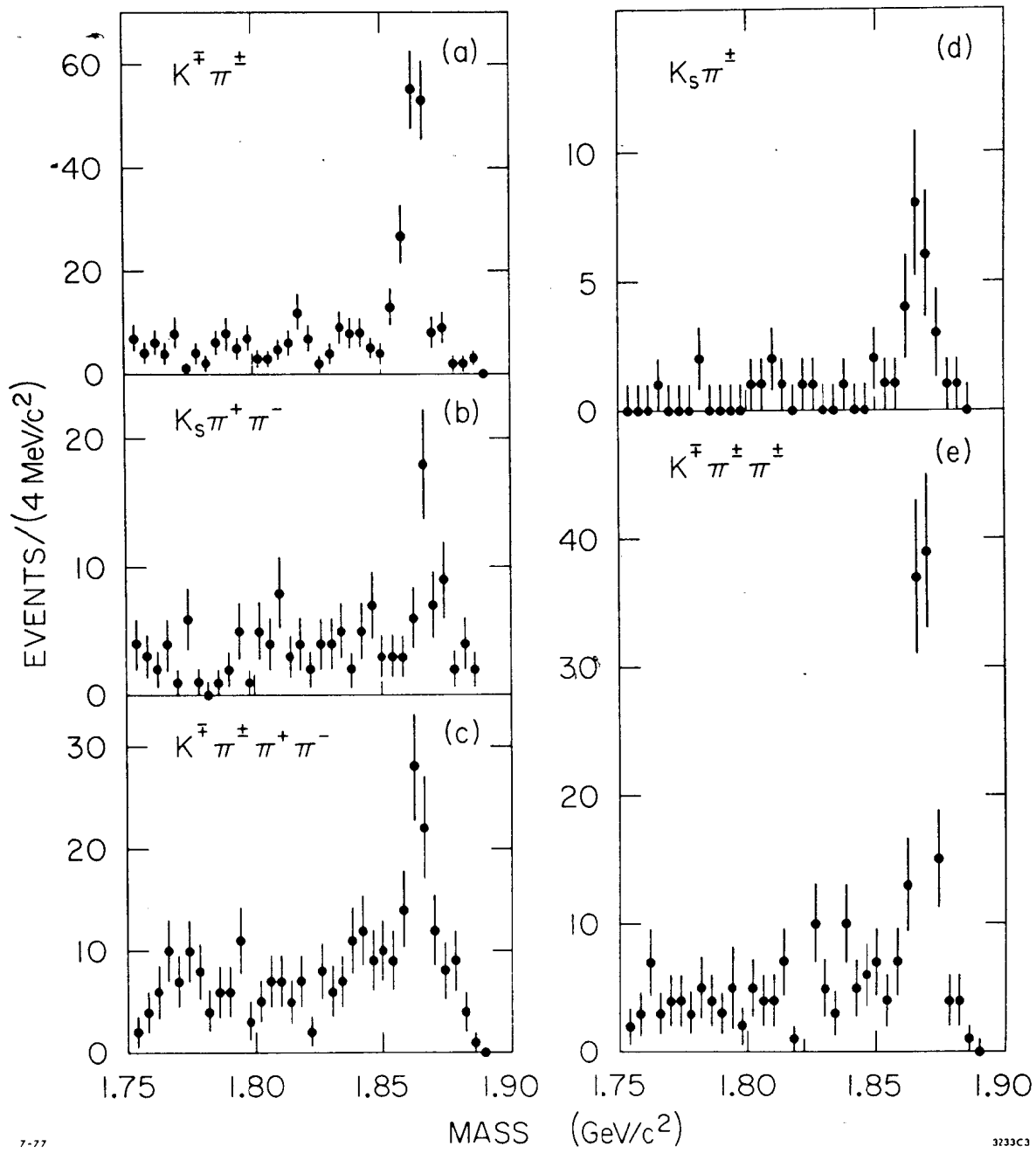


FIG. 4. Invariant mass spectra for various D decay modes at the  $\psi'$ .

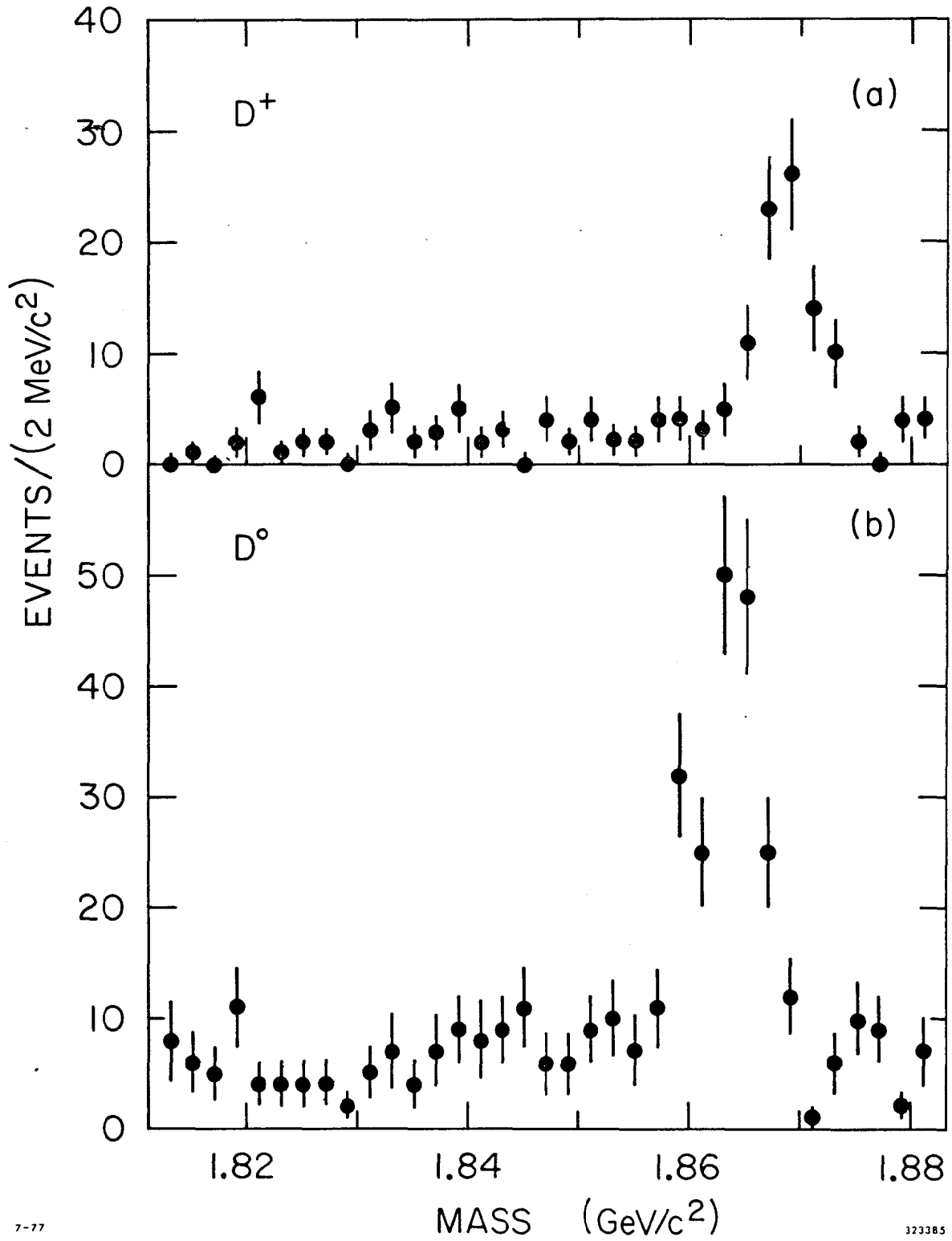


FIG. 5. Invariant mass spectra for the sum of all observed (a) D<sup>+</sup> and (b) D<sup>0</sup> decay modes.

a) We observe the  $D^0$  from  $D^{*0} \rightarrow D^0 \pi^0$  decay. Since the Q value of the reaction is small, the  $D^0$  carries off most of the  $D^{*0}$  momentum. Thus the detection of the  $D^0$  rather than the  $D^{*0}$  causes no real problem.

b) There is contamination from  $D^{*+} \rightarrow D^0 \pi^+$  and  $D^{*0} \rightarrow D^0 \gamma$  decays. Figure 6a shows the contributions to the  $D^0$  momentum spectrum. The problem here is to determine the center of peak B [ $D^{*0} \rightarrow D^0 \pi^0$ ] in the presence of peaks A [ $D^{*+} \rightarrow D^0 \pi^+$ ] and C [ $D^{*0} \rightarrow D^0 \gamma$ ].

The data and a fit to the data are shown in Fig. 6b. The  $D^{*0}$  mass is determined to be  $2006 \pm 1.5 \text{ MeV}/c^2$ . The uncertainty is larger here than it was for the  $D^0$  or  $D^+$  because of the difficulty of extracting the signal and because the fit is not perfect.

### C. $D^{*+}$ Mass

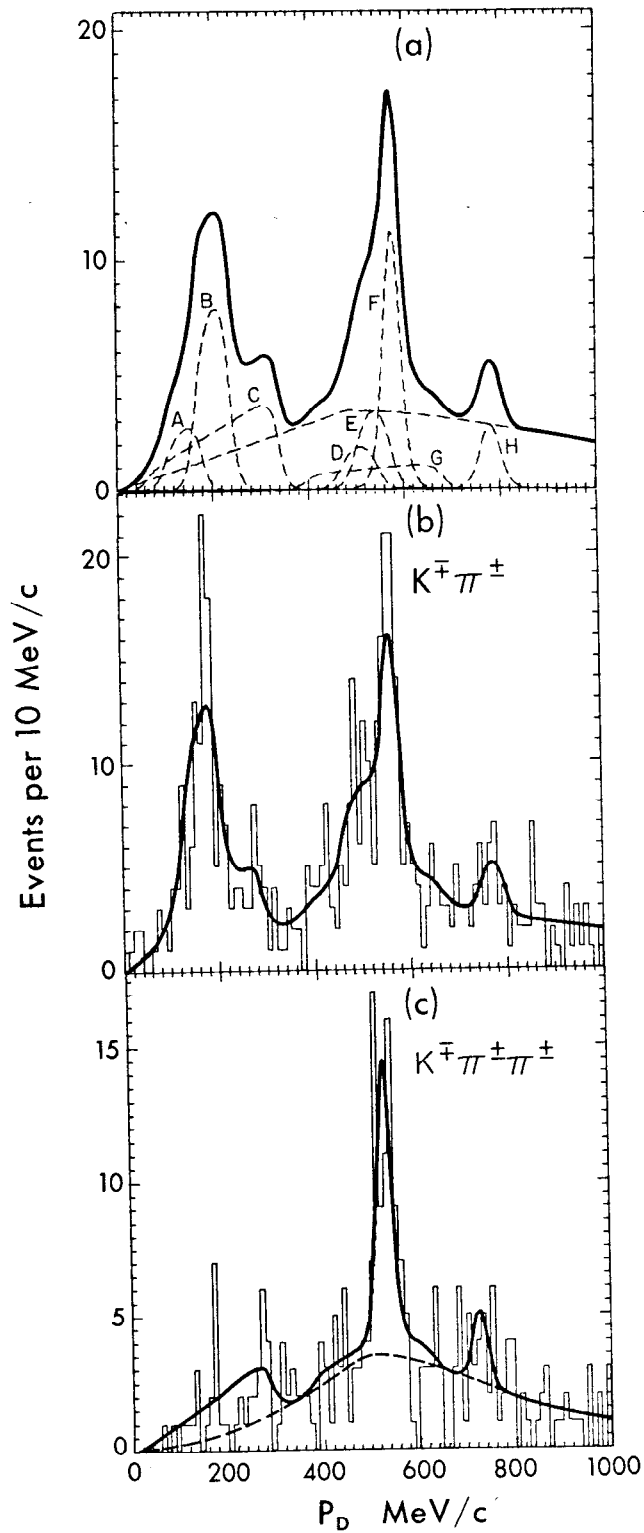
There are insufficient statistics to enable us to observe  $D^{*+} D^{*-}$  production at 4.028 GeV (see Fig. 6c), so another method is used to obtain the  $D^{*+}$  mass: We observe the  $D^{*+} \rightarrow D^0 \pi^+$  decay directly.<sup>3</sup> Since the Q value is small the  $\pi^+$  momentum will be only  $m_\pi/m_{D^{*+}}$  ( $\sim 7\%$ ) of the  $D^{*+}$  momentum. It is thus necessary to use high momentum  $D^{*+}$ 's from high energy data ( $\langle E_{c.m.} \rangle = 6.8 \text{ GeV}$ ) to obtain pions with enough momentum to be visible in the magnetic detector.

The kinematics in this case are not as transparent as they were in the previous cases, but the essential point is that the Q value determines the kinematics and even a crude measurement of the Q value translates into a very precise measurement of the  $D^{*+}$  mass. Figure 7 shows the  $D^{*+} - D^0$  mass difference in  $1 \text{ MeV}/c^2$  bins. The Q value is determined to be  $5.7 \pm 0.5 \text{ MeV}$  which, when combined with the  $D^0$  mass, yields a  $D^{*+}$  mass of  $2008.6 \pm 1.0 \text{ MeV}/c^2$ .

### D. Mass Differences and Q Values

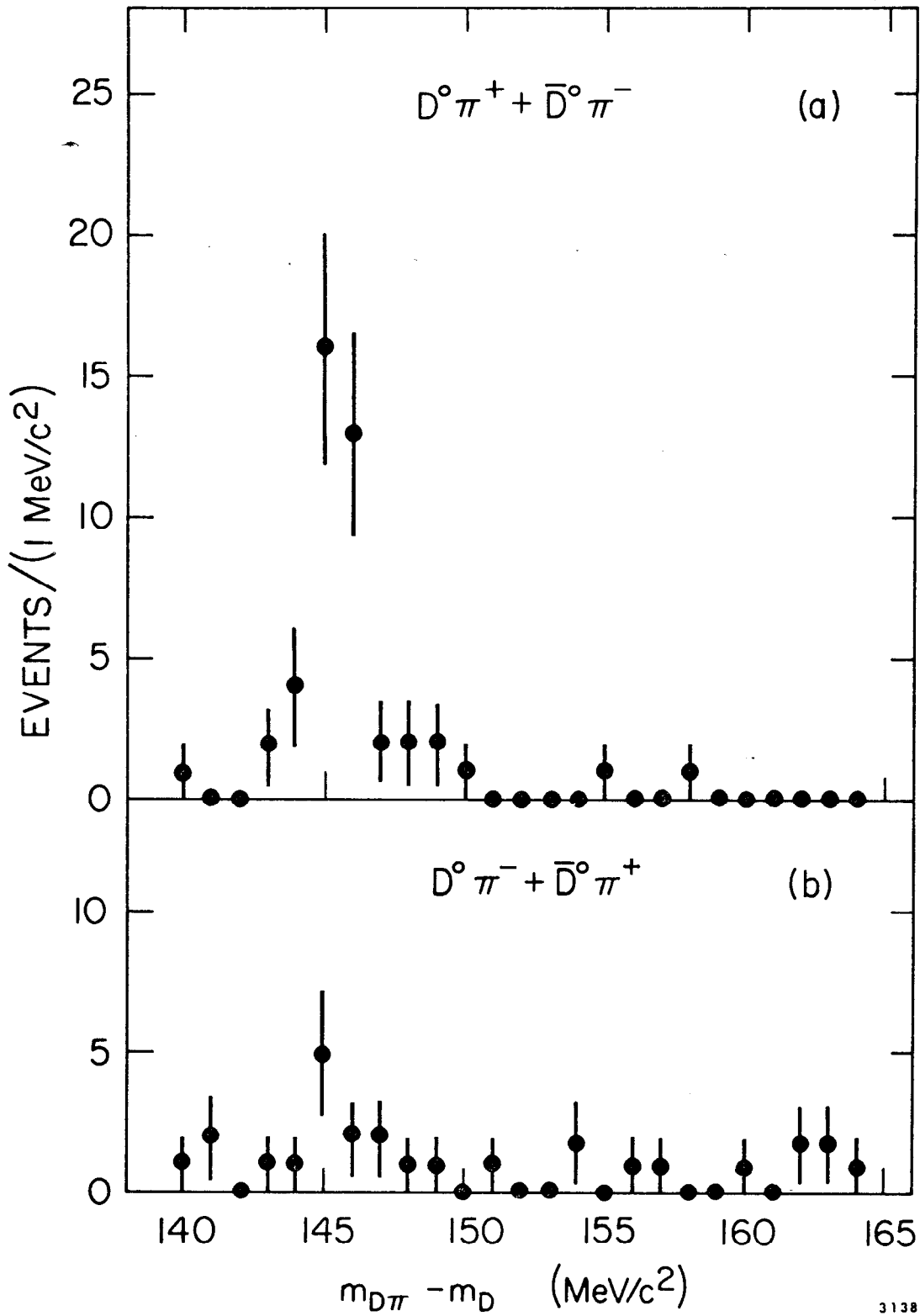
We previously gave the mass difference

$$\delta \equiv m_{D^+} - m_{D^0} = 5.1 \pm 0.8 \text{ MeV}/c^2 \quad (6)$$



XBL-776-1171

FIG. 6. D momentum spectra at 4.028 GeV for (b)  $D^0 \rightarrow K^- \pi^+ \pi^-$  and (c)  $D^\pm \rightarrow K^\mp \pi^\pm \pi^\pm$ . The solid curves represent an isospin constrained fit to the data. (a) shows the various contributions to the fit in (b). A, B, and C are contributions from  $D^* D^*$  production with A:  $D^{*+} \rightarrow D^0 \pi^+$ , B:  $D^{*0} \rightarrow D^0 \pi^0$  and C:  $D^{*0} \rightarrow D^0 \gamma$ . See Ref. 4 for remainder of key.



3138A5

FIG. 7.  $D\pi - D$  mass difference spectra for (a)  $D^0\pi^+$  and  $\bar{D}^0\pi^-$  combinations and (b)  $\bar{D}^0\pi^+$  and  $D^0\pi^-$  combinations.

We can now add

$$\delta^* \equiv m_{D^{*+}} - m_{D^{*0}} = 2.6 \pm 1.8 \text{ MeV}/c^2 \quad (7)$$

and

$$\delta - \delta^* = 2.5 \pm 2.4 \text{ MeV}/c^2 \quad (8)$$

The quantity  $\delta - \delta^*$  is an electromagnetic hyperfine splitting for which theoretical estimates vary between 0 and 3 MeV/c<sup>2</sup>.<sup>20</sup> The error given in Eq. 8 is somewhat larger than would be naively expected from Eqs. 6 and 7 because of correlations in the errors.

The Q values for  $D^* \rightarrow D\pi$  and  $D^* \rightarrow D\gamma$  are given in Fig. 8. The decay  $D^{*0} \rightarrow D^+\pi^-$  appears to be kinematically forbidden in the limit of zero  $D^{*0}$  width. Even allowing for finite  $D^*$  width, it cannot be an important decay mode.

#### E. $D^*$ Branching Fractions

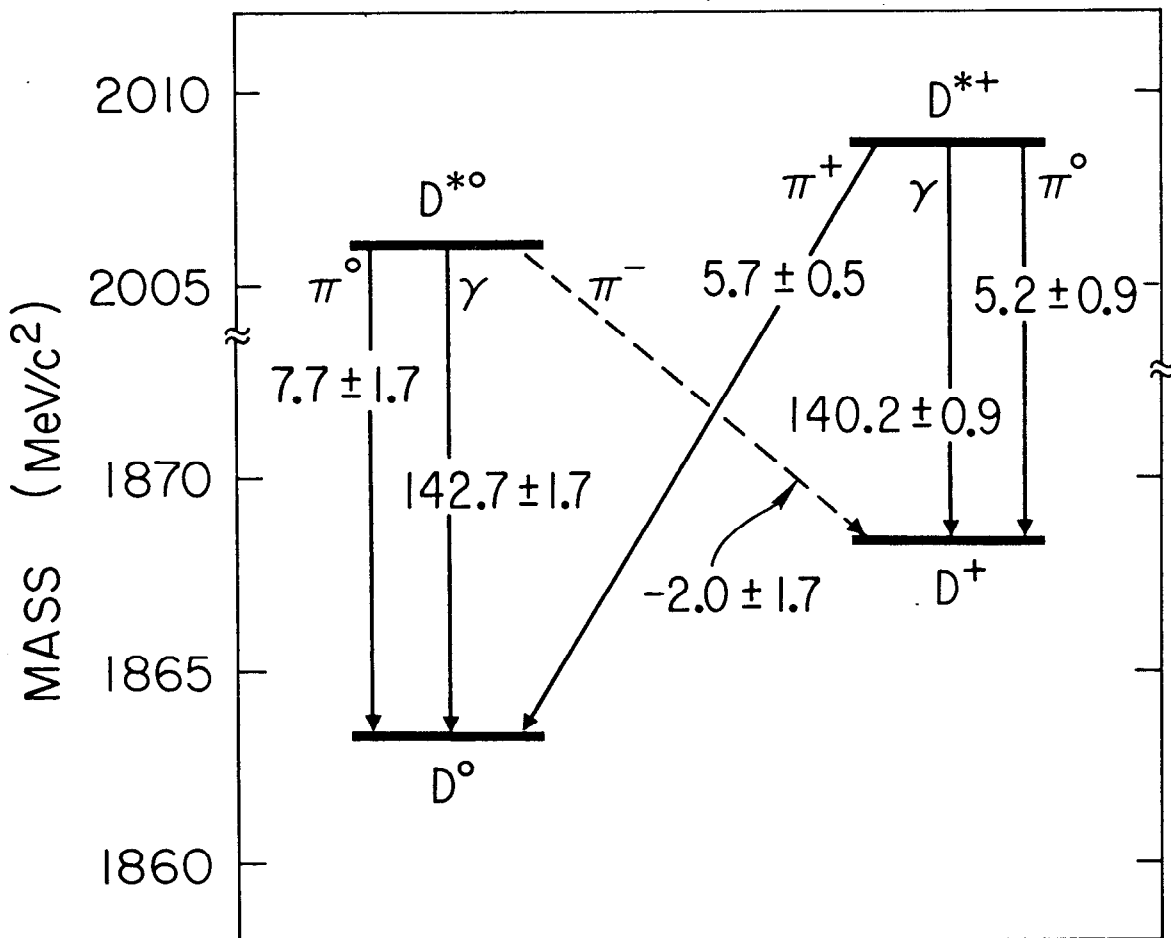
The  $D^{*0}$  branching fractions have been determined from the  $D^0$  momentum spectrum at 4.028 GeV by fitting the relative contribution of curves B and C in Fig. 7a.<sup>4</sup> The result is  $B(D^{*0} \rightarrow D^0\gamma) = 0.45 \pm 0.15$ .<sup>21</sup> The  $D^{*+}$  branching fractions were not well determined from the 4.028 GeV data due to insufficient statistics, but we can now calculate them using the  $D^* \rightarrow D\pi$  Q values and a few reasonable assumptions.

The inputs are:

- a) D and  $D^*$  masses, and
- b)  $B(D^{*0} \rightarrow D^0\gamma)$ .

The assumptions are:

- a) Isospin conservation in  $D^* \rightarrow D\pi$  decays,
- b)  $\Gamma(D^* \rightarrow D\pi)$  is proportional to  $p^3$  where p is the D momentum in the  $D^*$  rest frame, and
- c) the quark model prediction for  $\Gamma(D^* \rightarrow D\gamma)$ :<sup>22</sup>



7 77

3233A8

FIG. 8. Q values for  $D^* \rightarrow D$  transitions.

$$\frac{\Gamma(D^{*+} \rightarrow D^+\gamma)}{\Gamma(D^{*0} \rightarrow D^0\gamma)} = \frac{(\mu_c - \mu_{\bar{d}})^2}{(\mu_c - \mu_{\bar{u}})^2}, \quad (9a)$$

where  $\mu$  is a quark magnetic moment which we assume is inversely proportional to the quark mass. Thus,

$$\frac{\Gamma(D^{*+} \rightarrow D^+\gamma)}{\Gamma(D^{*0} \rightarrow D^0\gamma)} = \left( \frac{2 \frac{m_u}{m_c} - 1}{2 \frac{m_u}{m_c} + 2} \right)^2 \quad (9b)$$

taking  $m_d = m_u$ . The quark masses are not real masses and cannot be determined with any real accuracy. We will thus take two extreme cases to test the sensitivity of this assumption:  $m_u/m_c = m_\rho/m_\psi$  and  $m_u/m_c = 0$ .

We obtain

$$\frac{\Gamma(D^{*+} \rightarrow D^+\gamma)}{\Gamma(D^{*0} \rightarrow D^0\gamma)} = \begin{cases} 1/25 & \text{for } \frac{m_u}{m_c} = \frac{m_\rho}{m_\psi} \\ 1/4 & \text{for } \frac{m_u}{m_c} = 0. \end{cases} \quad (9c)$$

The results are given in Table II. Independent of the details of assumption (c),  $B(D^{*+} \rightarrow D^+\gamma)$  is small, and  $B(D^{*+} \rightarrow D^0\pi^+)$  is about twice as large as  $B(D^{*+} \rightarrow D^+\pi^0)$ . By accident, the total  $D^{*0}$  width is about equal to the  $D^{*+}$  width. The best experimental information on  $D^*$  widths comes from Fig. 7 from which we can deduce that  $\Gamma_{D^{*+}} < 2.0 \text{ MeV}/c^2$  at the 90% confidence level.<sup>3</sup>

TABLE II

$D^*$  branching fractions and widths. See the text for a discussion of the input data and the assumptions which were used.

	$D^{*0}$	$D^{*+}$ $\left(\frac{m_u}{m_c} = \frac{m_\rho}{m_\psi}\right)$	$D^{*+}$ $\left(\frac{m_u}{m_c} = 0\right)$
$B(D^{*+} \rightarrow D\pi^+)$	0	$0.68 \pm 0.08$	$0.63 \pm 0.09$
$B(D^{*+} \rightarrow D\pi^0)$	$0.55 \pm 0.15$	$0.30 \pm 0.08$	$0.27 \pm 0.07$
$B(D^{*+} \rightarrow D\gamma)$	$0.45 \pm 0.15$	$0.02 \pm 0.01$	$0.10 \pm 0.05$
$\Gamma(D^{*0})/\Gamma(D^{*+})$	---	$1.0 \pm 0.3$	$0.9 \pm 0.3$

#### IV. Inclusive Measurements

##### A. Relative Branching Fractions

The cross section times branching ratios ( $\sigma \cdot B$ ) for inclusive D production have been determined at  $E_{c.m.} = 3.774, 4.028, \text{ and } 4.414$  GeV. The data from the  $\psi''$  (i.e. 3.774 GeV) are shown in Fig. 4 and the data from 4.028 and 4.414 GeV are shown in Fig. 9.<sup>5</sup> The results are given in Table III. The relative  $D^0$  branching fractions from 3.774 GeV and 4.028 are in good agreement. The data from 4.414 are not in as good agreement, but as can be seen from Fig. 9, there are higher backgrounds at 4.414 than at lower energies and it is more difficult to extract the signal. No conclusive evidence for Cabbibo suppressed decays has been seen at any energy. There are upper limits given in Table III for  $E_{c.m.} = 4.028$  GeV which are consistent with the expected degree of suppression.

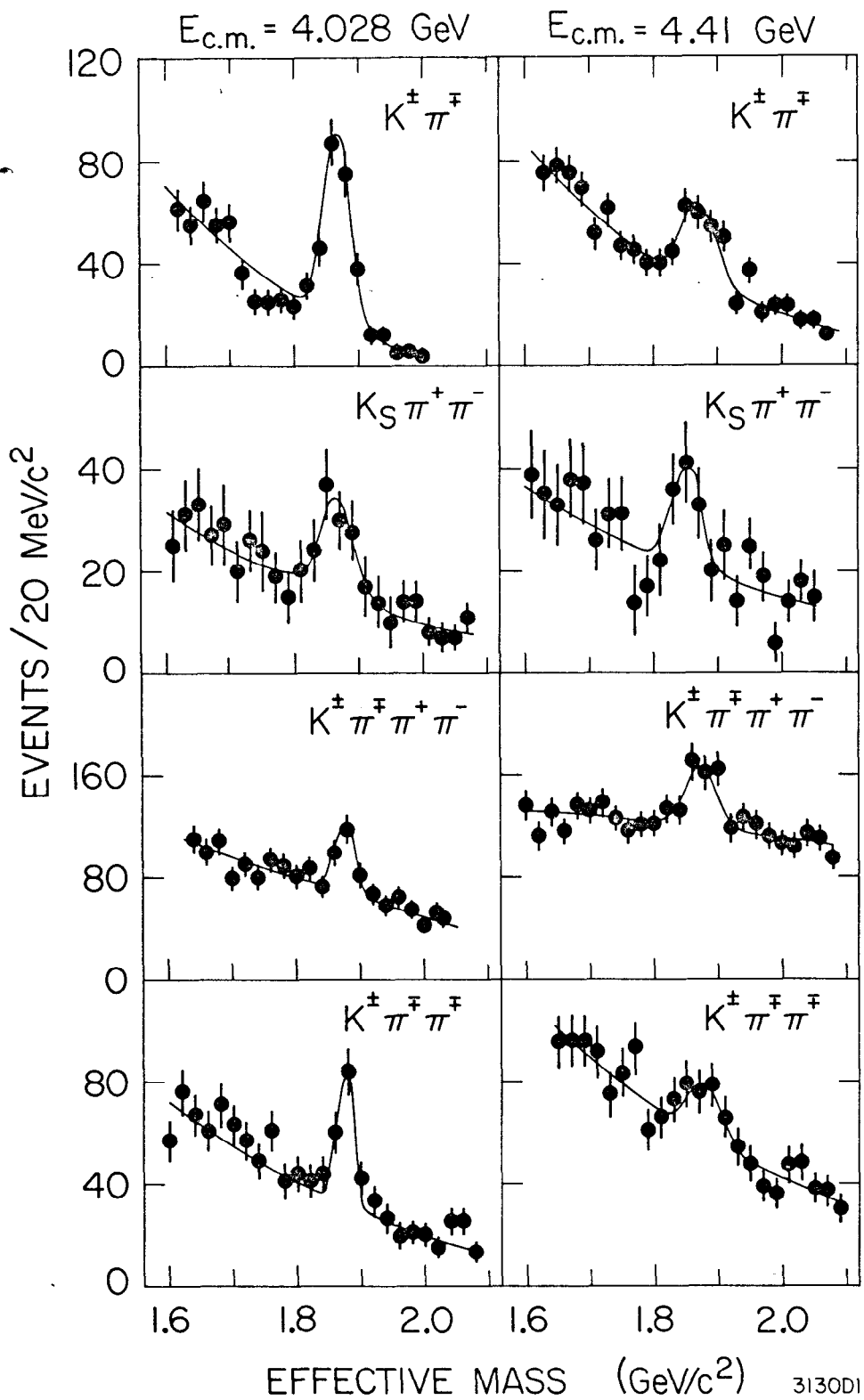


FIG. 9. Invariant mass spectra for various D decay modes at 4.028 and 4.414 GeV.

TABLE III

$\sigma \cdot B$  in nb for various D decay modes at three values of  $E_{c.m.}$

Mode	$E_{c.m.}$ (GeV)		
	3.774	4.028	4.414
$D^0$ $\bar{K}^+ \pi^-$	$0.27 \pm 0.05$	$0.57 \pm 0.11$	$0.30 \pm 0.09$
$\bar{K}^0 \pi^+ \pi^- + c.c.$	$0.44 \pm 0.11$	$1.09 \pm 0.30$	$0.91 \pm 0.34$
$\bar{K}^+ \pi^+ \pi^-$	$0.34 \pm 0.09$	$0.83 \pm 0.27$	$0.91 \pm 0.39$
$\pi^+ \pi^-$	---	$< 0.04$	---
$K^+ K^-$	---	$< 0.04$	---
Total $D^0$ observed modes	$1.05 \pm 0.15$	$2.49 \pm 0.42$	$2.12 \pm 0.53$
$D^+$ $\bar{K}^0 \pi^+ + c.c.$	$0.15 \pm 0.05$	$< 0.18$	---
$\bar{K}^+ \pi^+ \pi^-$	$0.34 \pm 0.05$	$0.40 \pm 0.10$	$0.33 \pm 0.12$
$\pi^+ \pi^+ \pi^-$	---	$< 0.03$	---

### B. Absolute Branching Fractions

In the  $\psi''$  we have for the first time a situation in which charm production is sufficiently simple that we can use measurements of the total cross section and of  $\sigma \cdot B$  for D decay modes to calculate absolute branching fractions.

The inputs are

- a)  $\sigma \cdot B$  measurements at the  $\psi''$  given in section IV.A, and
- b) the total cross section measurements in the vicinity of the  $\psi''$  given in section II.

The assumptions are

- a) The  $\psi''$  is a state of definite isospin, either 0 or 1. This assumption gives equal partial widths to  $D^0 \bar{D}^0$  and  $D^+ D^-$  except for phase

space factors.

b) The phase space factors are given by Eq. 2. The value of  $r$  is not known, but as  $r$  varies from 0 to infinity, the fraction of  $D^0 \bar{D}^0$  changes from 0.59 to 0.53. We can thus take this fraction to be  $0.56 \pm 0.03$ . The error due to the uncertainty in  $r$  is small compared to other systematic errors.

c)  $D\bar{D}$  is the only substantial decay mode of the  $\psi''$ . The rationale for this assumption was discussed in section II.

The results are given in Table IV. The  $\bar{K}^0 \pi^+$  decay mode of the  $D^+$  is comparable in size to the  $D^0 \rightarrow K^- \pi^+$  decay mode. This decay does not appear to be suppressed as was suggested from the analogue of octet enhancement in strangeness changing decays.<sup>23</sup>

TABLE IV

D branching fractions. See the text for a discussion of the input data and the assumption which were used.

	Mode	Branching fraction (%)
$D^0$	$K^- \pi^+$	$2.2 \pm 0.6$
	$\bar{K}^0 \pi^+ \pi^-$	$3.5 \pm 1.1$
	$K^- \pi^+ \pi^- \pi^+$	$2.7 \pm 0.9$
$D^+$	$\bar{K}^0 \pi^+$	$1.5 \pm 0.6$
	$K^- \pi^+ \pi^+$	$3.5 \pm 0.9$

### C. Comparison to the Statistical Model

It is instructive to compare the absolute branching fractions given in Table IV to the predictions of a statistical model. This model, due to Rosner,<sup>24</sup> uses a Poisson multiplicity distribution and, within each multiplicity, equal contributions from each isospin amplitude. There is no real

theoretical justification for this model and one should probably view its predictions with a certain degree of skepticism. Nevertheless, it can serve as a crude guide to the reasonableness of our measurements.

The statistical model predictions are given in terms of the ratio of a given state to the sum of all states of the form  $K + n\pi$ . Therefore we will define  $f_{Kn\pi}$  to be the ratio

$$f_{Kn\pi} = \frac{\Sigma B(D \rightarrow K + n\pi)}{B(D \rightarrow \text{all})} . \quad (10)$$

In addition to  $K + n\pi$ , "all" will include  $K\eta + n\pi$ , semi-leptonic decays, and Cabibbo suppressed decays. In Table V we list the prediction times  $f_{Kn\pi}$  divided by the measurement. We expect this quantity to be unity, but it appears that this will be true only if  $f_{Kn\pi}$  is about 0.35. This value seems low as we would expect a value of 0.6 or higher if the semileptonic branching fractions are of the order of 0.2 for the sum of electronic and muonic modes.<sup>1</sup> We may have here the start of a D branching ratio crisis, but I think we should reserve judgement until some modes involving  $\pi^0$ 's are measured.

TABLE V

Comparison of the absolute D branching fractions from Table IV with the statistical model of Ref. 24. See text for the definition of  $f_{Kn\pi}$ .

	mode	prediction/measurement
$D^0$	$K^- \pi^+$	$(2.7 \pm 0.7) f_{Kn\pi}$
	$\overline{K^0} \pi^+ \pi^-$	$(3.4 \pm 1.1) f_{Kn\pi}$
	$K^- \pi^+ \pi^- \pi^+$	$(2.6 \pm 0.9) f_{Kn\pi}$
$D^+$	$\overline{K^0} \pi^+$	$(8.7 \pm 3.5) f_{Kn\pi}$
	$K^- \pi^+ \pi^+$	$(2.9 \pm 0.7) f_{Kn\pi}$

D. Charm Production at 4.028 and 4.414 GeV

With the absolute branching fractions from Table IV we are now in a position to calculate the amount of charm production at two of the prominent peaks in the 4 GeV region.

The inputs are

- a)  $\sigma \cdot B$  from Table III,<sup>5</sup> and
- b)  $B$  from Table IV.

There are no additional assumptions to those already used in constructing Table IV.

We define  $R_D = \sigma_D / (2\sigma_{\mu\mu})$ . The factor of 2 in the denominator takes into account the fact that charmed particles are produced in pairs, so that  $R_D$  can be directly compared to the total hadronic  $R$ . In particular, we compare it to

$$R_{\text{new}} \equiv R - R_{\text{old}} - R_{\tau} \quad (11)$$

where  $R$  is taken from measurements of the total hadronic cross section,<sup>11</sup>  $R_{\text{old}}$  (2.6) is taken from measurements of the total hadronic cross section below charm threshold,<sup>6</sup> and  $R_{\tau}$  is the theoretical expression for the production of a 1.9 GeV/c<sup>2</sup> mass lepton.

$$R_{\tau} = \frac{1}{2}\beta(3 - \beta^2) \quad (12)$$

If D's and  $\tau$ 's are the only new particles being produced then  $R_{\text{new}}$  should equal  $R_D$ . If the production of F's, charmed baryons, or even other new particles are sizable, then  $R_{\text{new}}$  will be larger than  $R_D$ .

The results are given in Table VI.  $R_{D^0}$  is calculated from all observed  $D^0$  modes and also from just the better-measured  $K^{\mp}\pi^{\pm}$  mode. At 4.028 GeV these two measurements are consistent and  $R_{\text{new}}$  is consistent with being equal to  $R_D$ . At 4.414 GeV the two measurements differ somewhat, but nevertheless it is clear that whatever else may be happening

at 4.414 GeV, most of the excess cross section is going into D production.<sup>25</sup>

We shall return to a discussion of  $R_{D^\pm}^\pm/R_D$  in section IV.F.

TABLE VI

Charm production at 4.028 and 4.414 GeV. See text for definitions and a discussion of the input data and assumptions which were used.

	4.028 GeV		4.414 GeV	
	all $D^0$ modes	$K^+\pi^-$ only	all $D^0$ modes	$K^+\pi^-$ only
$R_{D^0}$	$2.8 \pm 0.7$	$2.4 \pm 0.9$	$2.8 \pm 0.9$	$1.5 \pm 0.6$
$R_{D^\pm}^\pm$	$1.1 \pm 0.4$	$1.1 \pm 0.4$	$1.1 \pm 0.5$	$1.1 \pm 0.5$
$R_D$	$3.9 \pm 0.8$	$3.5 \pm 0.9$	$3.9 \pm 1.0$	$2.6 \pm 0.8$
$R_{\text{new}}$	$3.4 \pm 1.1$	$3.4 \pm 1.1$	$2.7 \pm 1.1$	$2.7 \pm 1.1$
$R_{D^\pm}^\pm/R_D$	$0.28 \pm 0.09$	$0.31 \pm 0.10$	$0.28 \pm 0.11$	$0.42 \pm 0.14$

### E. Charm Production at High Energy

The calculation of charm production in the high energy continuum is not as straight forward as it was at 4.028 and 4.414 GeV because

- a) There are no measurements of  $D^+$  production in this region, and
- b) The best measurements of  $D^0$  production are somewhat incomplete and indirect.

However, there is just enough information to justify a crude calculation.

The inputs are

- a)  $\sigma_{D^{*\pm}} \cdot B(D^{*+} \rightarrow D^0 \pi^+) \cdot B(D^0 \rightarrow K^-\pi^+) = 13 \pm 4 \text{ pb},^3$
- b)  $(25 \pm 9)\%$  of  $D^0$  production comes from  $D^{*+}$  production,<sup>3</sup> and
- c)  $B(D^0 \rightarrow K^-\pi^+)$  from Table IV.

Due to the techniques employed in Ref. 3, inputs (a) and (b) refer only to  $D^0$ 's with momenta greater than 1.5 GeV/c. We shall thus only be able

to calculate a lower limit on  $R_D$ , although there is likely to be only a small amount of low momentum D production.

The assumptions are

- a) Equal production of charged and neutral  $D^*$ 's, and
- b) Except for  $D^*$  decay, equal production of charged and neutral D's.

The results for  $\langle E_{c.m.} \rangle = 6.8$  GeV are

$$R_D \geq 0.9 \begin{matrix} + 0.7 \\ - 0.5 \end{matrix}, \quad (13a)$$

$$R_{new} = 1.7 \pm 0.8, \text{ and} \quad (13b)$$

$$R_{\frac{+}{D^-}}/R_D = 0.33 \pm 0.08. \quad (13c)$$

These results are consistent with  $R_{new} = R_D$ , but also allow for a reasonable amount of F and charmed baryon production.

F. Alternate Calculation of  $R_{\frac{+}{D^-}}/R_D$  at 4.028 GeV

In section IV.D. we calculated  $R_{\frac{+}{D^-}}/R_D$  using relative and absolute branching ratios as inputs. We can check the consistency of our measurements by calculating this quantity at 4.028 GeV by an almost orthogonal technique.

The inputs are

- a)  $D^*$  branching fractions from Table II, and
- b) The relative  $D^{*0}\overline{D^{*0}}$ ,  $D^{*0}\overline{D^0}$ , and  $D^0\overline{D^0}$  production rates.<sup>4</sup>

The assumptions are

- a) The  $\psi(4030)$  is a state of definite isospin, either 0 or 1, so that there is equal production of charged and neutral D's and  $D^*$ 's, except for phase space factors. This assumption is somewhat questionable; it has been suggested that the  $\psi(4030)$  may have mixed isospin.<sup>26</sup>

- b) The phase space factor for  $D^* \overline{D^*}$  production is proportional to

$$p_{D^*}^3$$

The result is

$$R_{D^+}/R_{D^-} = 0.25 \pm 0.15, \quad (14)$$

which is consistent with the determinations of  $0.28 \pm 0.09$  and  $0.31 \pm 0.10$  from Table VI.

It is clear from these measurements that the fraction of charged D production at 4.028 GeV is significantly smaller than that at 3.774 GeV where we have assumed  $R_{D^+}/R_{D^-} = 0.44 \pm 0.03$ . In the near future one should be able to combine this result with inclusive lepton production at 4.028 and 3.774 GeV to calculate the ratio of  $D^+$  to  $D^0$  semileptonic branching fractions. Since semileptonic decays are  $\Delta I = 0$  transitions, this ratio is the inverse of the ratio of  $D^+$  to  $D^0$  lifetimes.<sup>27</sup>

#### V. Tagged Events

With the discovery of the  $\psi''$ , it becomes possible for the first time to "tag" charmed particle decays. For example, if we detect a  $D^0$  decay into  $K^- \pi^+$  in a  $\psi''$  decay, then we are also looking, essentially without bias, at a  $\overline{D^0}$  decay where the  $\overline{D^0}$  has a momentum of 300 MeV/c in a known direction.

#### A. Decays With All Charged Particles

In section IV.B. we determined absolute D branching fractions by employing some very reasonable assumptions about the nature of  $\psi''$ . We can now check these assumptions by using tagged events to measure D branching fractions.

We use the five decay modes shown in Fig. 4 as the tagging decays and look for events in which all or all but one of the decay products of the other D are detected. There are 194 tagging  $D^0$  decays and 82 tagging  $D^+$  decays.

We find eight cases of  $K^{\bar{+}}\pi^{+}$  or  $K^{\bar{+}}\pi^{-}\pi^{+}\pi^{-}$  decay opposite the tagging decays. These eight cases come from six events because in two cases both halves of the event tag each other, and such events must be counted twice. Correcting for detection and triggering efficiencies, these events give

$$B(D^0 \rightarrow K^{\bar{+}}\pi^{+} \text{ or } K^{\bar{+}}\pi^{-}\pi^{+}\pi^{-}) = (6.2 \pm 2.7)\% \quad (15)$$

which is consistent with the value of  $(4.9 \pm 1.1)\%$  from Table IV.

There are two cases of a  $K^{\bar{+}}\pi^{+}\pi^{-}$  decay opposite from a tagging  $D^{\bar{+}}$  decay, each from a separate event. These two events give

$$B(D^{\bar{+}} \rightarrow K^{\bar{+}}\pi^{+}\pi^{-}) = (3.4 \pm 2.4)\% \quad , \quad (16)$$

which is in clearly fortuitous agreement with the value of  $(3.5 \pm 0.9)\%$  from Table IV.

We can now turn these results around and use them to calculate  $\psi''$  branching fractions without the aid of any assumptions.

The inputs are

- a)  $\sigma \cdot B$  for D decays at the  $\psi''$  (Table III),
- b) B for D decays from the tagged events (Eqs. 15 and 16), and
- c)  $\psi''$  total cross section measurements.<sup>6</sup>

The results are given in Table VII along with the values which were assumed in section IV.B. The measurements are consistent with the assumed values.

---

Table VII

$\psi''$  branching fractions in per cent. See the text for a discussion of the input data.

	B measured	B (assumed in Sec. IV.B.)
$\psi'' \rightarrow D^0 \bar{D}^0$	$44 \pm 22$	$56 \pm 3$
$\psi'' \rightarrow D^{\bar{+}} D^{-}$	$44 \pm 33$	$44 \pm 3$
$\psi'' \rightarrow D \bar{D}$	$88 \pm 40$	100

### B. Decays With One Missing Neutral

We can also look for events with a charged kaon, another charged particle, and a missing, near zero-mass, neutral particle opposite a tagging  $D^0$  decay. These decays could be  $D^0 \rightarrow K^{\mp} \pi^{\pm} \pi^0$ ,  $D^0 \rightarrow K^{\mp} e^{\pm} \nu$ , or  $D^0 \rightarrow K^{\mp} \mu^{\pm} \nu$  modes, which we shall designate as  $D_{\pi 3}$ ,  $D_{e 3}$ , and  $D_{\mu 3}$  for short. There are ten cases of these events, which leads to

$$B(D_{\pi 3}) + B(D_{e 3}) + B(D_{\mu 3}) = (11.7 \pm 4.1)\% \quad . \quad (17)$$

Unfortunately it is quite difficult to distinguish between,  $D_{\pi 3}$  and  $D_{\ell 3}$  decays in the magnetic detector because

- a) the leptons often have low momentum and are not discriminated from pions, and
- b) low energy  $\pi^0$ 's are difficult to detect.

Figure 10 is a computer reconstruction of the one event, out of these 10 events, most likely to be a  $D_{\ell 3}$  decay. One is viewing the magnetic detector along the beam. The short closed boxes represent trigger counters and the long open boxes represent shower counters which have fired. Tracks labeled with the subscript 1 are from the tagging decay while those labeled 2 are from the other D decay. The tagging decay here is  $D^0 \rightarrow K^- \pi^+ \pi^- \pi^+$ . Note that the 250 MeV/c  $\pi^+$  in the upper right hand corner backscatters and eventually reaches the trigger counter to the right of the  $K^-$ . Although the computer does not track the backscatter the full distance, the trigger counter in question fires 15 nsec late which is consistent with this hypothesis. There are two charged particles left in the event. The positively charged particle is unambiguously identified as a kaon by time-of-flight and the 650 MeV/c negatively charged particle is identified as a muon by the firing of a spark chamber located behind the flux return. There is about a 12% probability that a pion of this momentum would penetrate

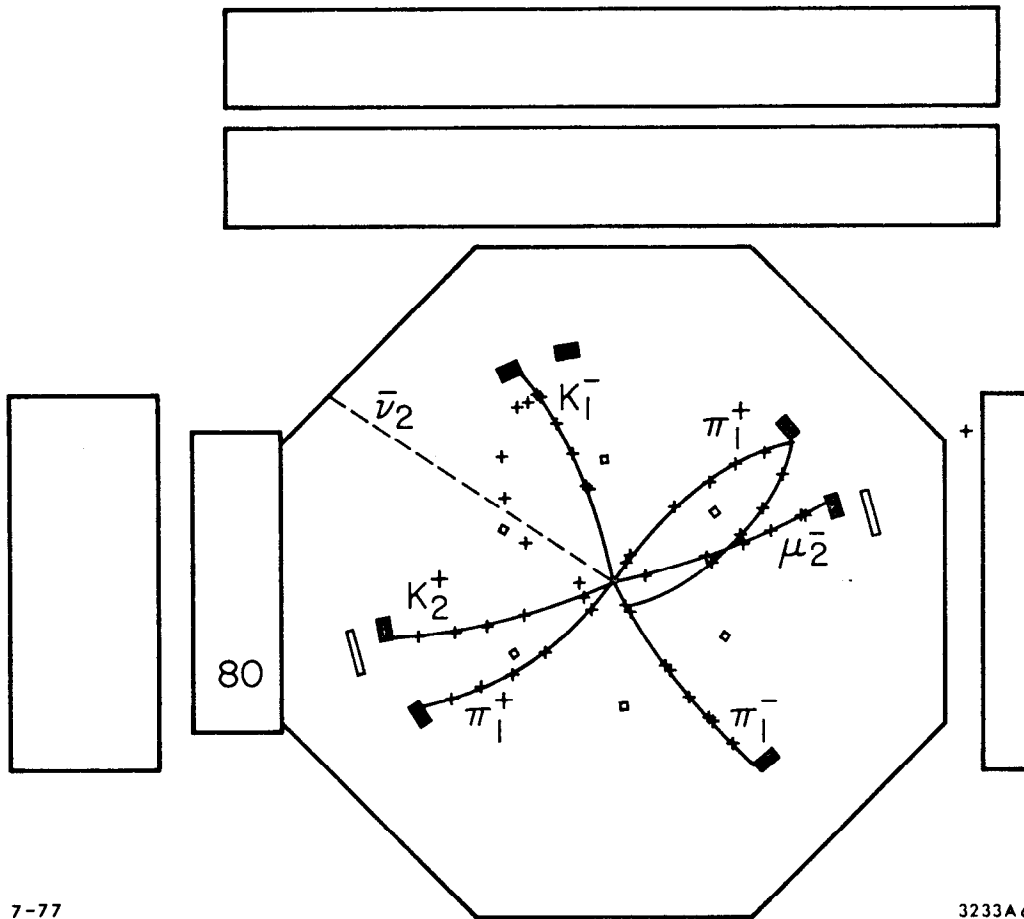
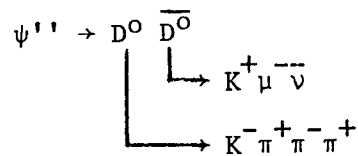


FIG. 10. An event which is interpreted as



See text for discussion.

the flux return and be misidentified as a muon. There is approximately 500 MeV/c of missing momentum in the direction indicated by " $\bar{\nu}_2$ ". The missing energy in the event is consistent with being equal to the missing momentum and within errors one cannot determine from missing mass whether the missing neutral is a neutrino or  $\pi^0$ . If we assume that the missing neutral is a  $\pi^0$ , then in the worst case at least one of the decay photons must be in the active area of the shower counters and deposit at least 200 MeV of energy. The probability of the shower counters failing to fire on a 200 MeV photon is between 10 and 20%. Thus, everything else being equal, this event is 50 to 100 times more likely to be a  $D_{\mu 3}$  decay than a  $D_{\pi 3}$  decay. I have selected this event for a detailed discussion not so much to convince you that it is a  $D_{\ell 3}$  decay as to demonstrate the difficulty of distinguishing these decays in our present detector.

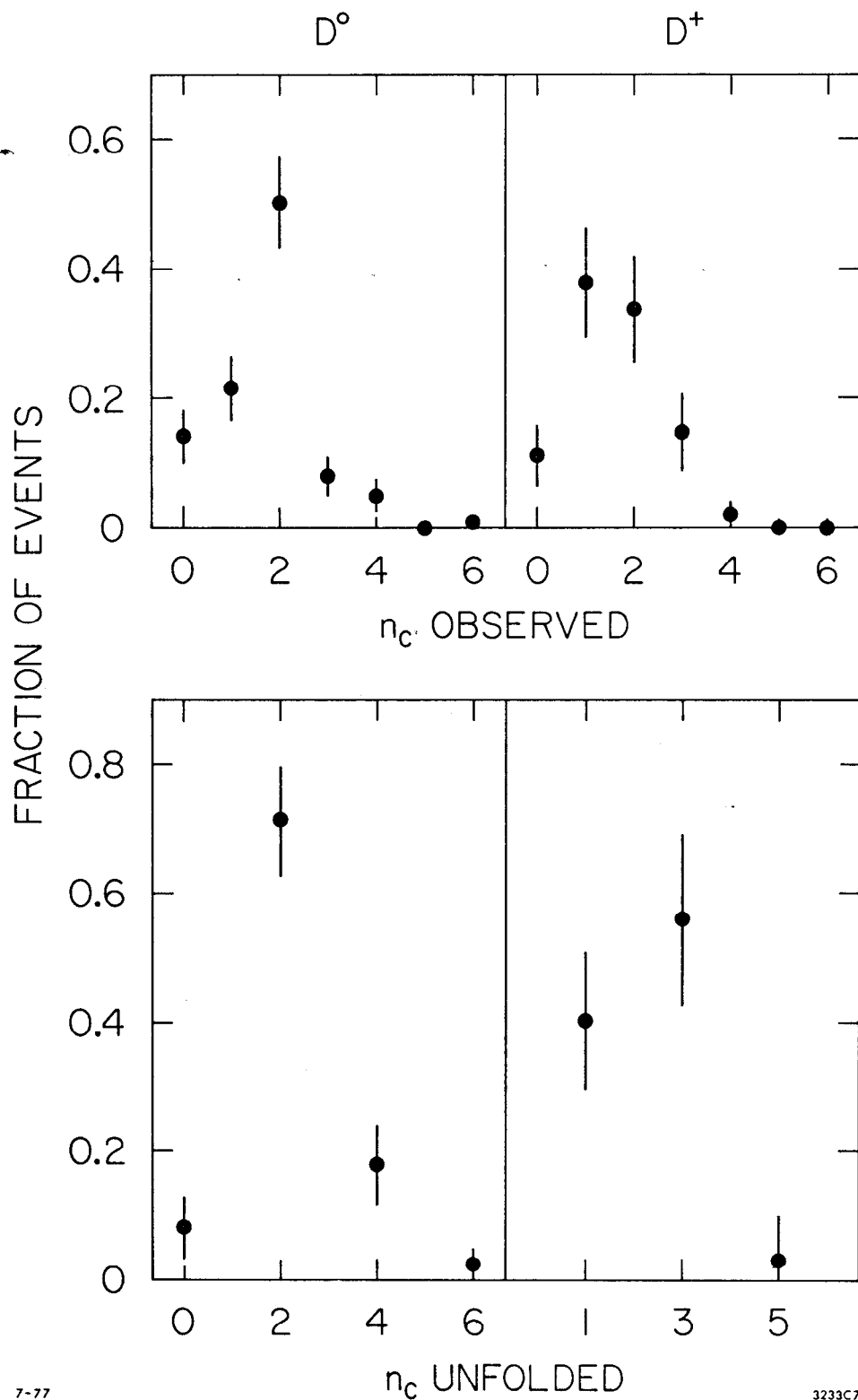
### C. Charged Multiplicity in D Decays

To determine the charged multiplicities in D decays, we count the charged particles opposite a tagging decay and use a Monte Carlo calculation of efficiencies to unfold the true distributions from the observed distributions.<sup>28</sup> In this preliminary analysis we have used only the  $K^+ \pi^-$  and  $K^+ \pi^+ \pi^-$  modes as tagging decays. Backgrounds, which are typically about 10%, have been explicitly subtracted from the data. No attempt has been made to identify neutral kaons so that a  $K_S^0$  decaying to two charged pions will count as two charged particles.

The raw data are displayed in the top portion of Fig. 11 and the unfolded data are displayed in the bottom portion.  $D^0$ 's decay primarily to two charged particles, while  $D^+$ 's decay to roughly equal numbers of one and three charged particles. The mean charged multiplicities are

$$\langle n_c \rangle_{D^0} = 2.3 \pm 0.2 \quad (18a)$$

$$\langle n_c \rangle_{D^+} = 2.3 \pm 0.3 \quad (18b)$$



7-77

3233C7

FIG. 11. Observed and true (unfolded) charged multiplicities for D decays.

The statistical model assumed somewhat higher charged multiplicities, typically about 2.7.

D. Two-prong  $D\bar{D}$  Decays

Events in which only two charged particles are produced are of special interest experimentally because

- a) there is background in two-prong events from QED processes,
- b) they have a much lower detection efficiency in the magnetic detector and most other detectors, and
- c)  $\tau^+\tau^-$  decays occur primarily in two-prong events.

We can calculate the fraction of  $D\bar{D}$  decays that go into two charged particles directly from the data in Fig. 11:

$$D^0\bar{D}^0 : 2f_0f_2 = (11 \pm 7)\% \quad (19a)$$

$$D^+D^- : f_1^2 = (17 \pm 8)\% . \quad (19b)$$

Here  $f_n$  represents the fraction of decays to  $n$  charged particles. The fractions of two charged particle events given by Eq. 19 are not vastly different from the overall fraction of two prong events. We thus expect to see the same type of variation with energy in the two prong cross section as in the multiprong cross section.

Semileptonic decays of  $D$ 's and leptonic decays of  $\tau$ 's are often separated experimentally by multiplicity: the  $D$ 's are presumed to decay primarily into events with four or more charged particles while  $\tau$ 's are presumed to decay primarily into events with two charged particles.<sup>29</sup>

It is thus important to measure the extent to which semileptonic  $D$  decays can occur in two-charged-prong events. We do not presently have enough information to determine this but we can set upper limits by assuming that semileptonic decays always occur in the lowest possible charged multiplicities.

For  $D^0\bar{D}^0$  decays the lowest charged multiplicity is clearly two, therefore

$$D^0\bar{D}^0 \text{ 2-prong lepton fraction} < f_0 \\ < 13\% \text{ at } 1\sigma \text{ c.l.} \quad (20a)$$

For  $D^+D^-$  decays one might expect that the upper limit is just  $f_1$ .

However we can obtain a better limit if we assume that Cabbibo suppressed decays are unimportant. Then the simplest semileptonic decay is  $D^+ \rightarrow K^0\ell^+\nu$ . The  $K^0$  looks like zero prongs two-thirds of the time and like two prongs one-third of the time. Therefore

$$D^+D^- \text{ 2-prong lepton fraction} < 0.66 f_1 \\ < 34\% \text{ at } 1\sigma \text{ c.l.} \quad (20b)$$

#### E. Neutral and Charged Kaon Production in $D^+$ Decays

If we assume that Cabbibo suppressed decays are unimportant and if  $f_1 > 0.33$ , then  $D^+$ 's must decay to neutral kaons more often than they decay to charged kaons. The proof is straightforward:  $D^+$ 's decay to  $K^-$ 's, so to conserve charge a  $D^+$  decay to a charged kaon must contain at least three charged particles. A  $D^+$  decay to a neutral kaon will appear to be a three-or-more charged particle decay at least one-third of the time because the kaon will decay into  $\pi^+\pi^-$ . Therefore, if  $D^+$ 's decayed equally to neutral and charged kaons, at least two-thirds of decays would have three-or-more charged particles and  $f_1 < 0.33$ .

From Fig. 11,  $f_1 = (41 \pm 11)\%$ , so it is likely that the condition  $f_1 > 0.33$  is met, but it is not conclusive.

It is often assumed that overall there should be equal numbers of charged and neutral kaons from charmed particle decays. This need not be the case and, in fact, is not even true in the statistical model.<sup>24</sup> The predictions of this model are shown in Table VIII. The symmetry in the semileptonic decays is a consequence of the fact that these decays are  $\Delta I = 0$  transitions. It is clear that if there are equal numbers

of neutral and charged D's produced then in this model overall there would be more neutral kaons than charged kaons in their decays.

Table VIII

Fraction of neutral and charged kaons in D decays according to the statistical model (Ref. 24).

	$\overline{K}^0$	$K^-$
$D^0$ nonleptonic	0.54	0.46
$D^+$ nonleptonic	0.68	0.32
$D^0$ semileptonic	0.38	0.62
$D^+$ semileptonic	0.62	0.38

VI. Epilogue: A Beautiful Event

If you study Fig. 11 carefully, you will notice that in the raw charged multiplicity for tagged  $D^0$  decays the number of five-prong events is zero, but not the number of six-prong events. In fact, exactly one decay with six charged particles was detected. When we examined this event, we were amazed to discover that there was, within errors, no missing momentum or energy. This event, which is shown in Fig. 12, is

$$e^+e^- \rightarrow \psi' \rightarrow D^0 \overline{D}^0 \quad (21)$$

$\begin{array}{l} \rightarrow K_S^+ \pi^+ \pi^- \pi^+ \pi^- \\ \rightarrow K^- \pi^+ \end{array}$

If one were so foolhardy as to calculate a branching fraction for  $D^0 \rightarrow \overline{K}^0 \pi^+ \pi^- \pi^+ \pi^-$  from this single event, one would obtain the clearly absurd value of about 25%. We were thus very lucky to be able to see this beautiful decay.

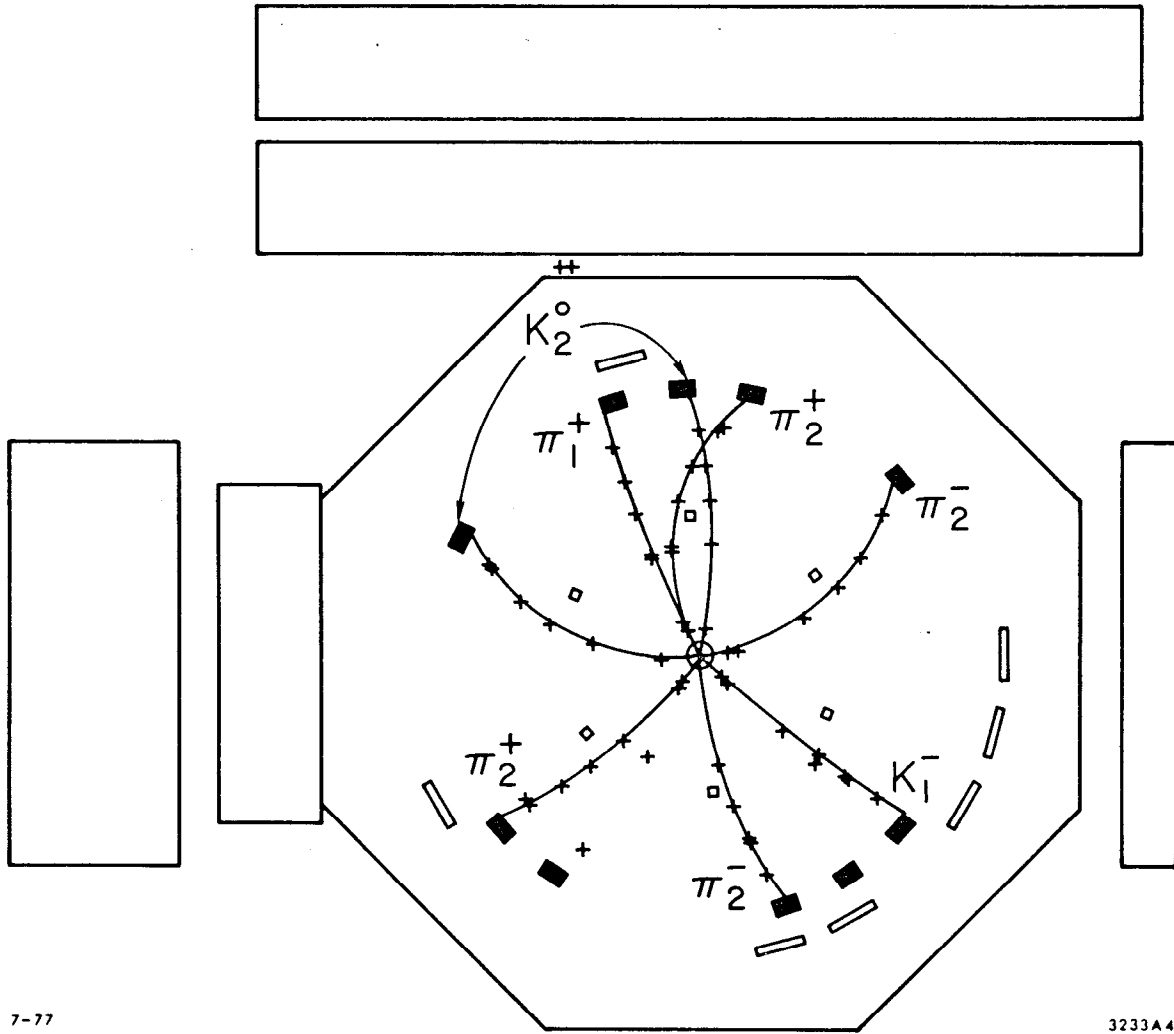
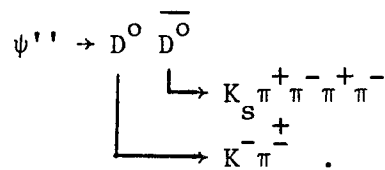


FIG. 12. An event which is interpreted as



The extra trigger and shower counters have presumably been fired by secondary interactions. The time-of-flight information from the extra trigger counters indicates that they were not fired by prompt particles.

## References

1. Semi-leptonic decays are discussed by W. De Boer, R.J. Madaras, and J. Kirz in these proceedings.
2. J.-E. Augustin et al., Phys. Rev. Lett. 34, 233(1975); G.J. Feldman and M.L. Perl, Phys. Rep. 19C, 233(1975), Appendix A; F. Vannucci et al., Phys. Rev. D15, 1814(1977); A. Barbaro-Galtieri et al., SLAC report number SLAC-PUB-1976 (1977).
3. G.J. Feldman et al., Phys. Rev. Lett. 38, 1313(1977).
4. G. Goldhaber et al., SLAC report number SLAC-PUB-1973 (1977).
5. M. Piccolo et al., SLAC report number SLAC-PUB-1978 (1977).
6. P.A. Rapidis et al., SLAC report number SLAC-PUB-1959 (1977).
7. Members of the SP26 collaboration are A. Barbaro-Galtieri, J.M. Dorfan, R. Ely, G.J. Feldman, J.M. Feller, A. Fong, B. Gobbi, G. Hanson, J.A. Jaros, B.P. Kwan, P. Lecomte, A.M. Litke, D. Lüke, R.J. Madaras, J.F. Martin, T.S. Mast, D.H. Miller, S.I. Parker, M.L. Perl, I. Peruzzi, M. Piccolo, T.P. Pun, P.A. Rapidis, M.T. Ronan, R.R. Ross, B. Sadoulet, D.L. Scharre, T.G. Trippe, V. Vuillemin, and D.E. Yount. Much of the analysis of the unpublished SP26 data presented here is work of I. Peruzzi and M. Piccolo.
8. H.K. Nguyen et al., Phys. Rev. Lett. 39, 262(1977) and unpublished SP26 data.
9. J.E. Wiss et al., Phys. Rev. Lett. 37, 1531(1976).
10. J.-E. Augustin et al. Phys. Rev. Lett. 34, 764(1975).
11. J. Siegrist et al., Phys. Rev. Lett. 36, 700(1976).
12. H.L. Lynch in Proceedings of the International Conference on the Production of Particles with New Quantum Numbers, University of Wisconsin, Madison, Wisconsin, April 22-24, 1976, p. 20.
13. J.D. Jackson, Nuovo Cimento 34, 1645(1964); A. Barbaro-Galtieri in Advance in Particle Physics, edited by R.L. Cool and R.L. Marshak (Wiley, New York), Vol. II, 1968.
14. A.M. Boyarski et al., Phys. Rev. Lett. 34, 1357(1975).
15. V. Lüth et al., Phys. Rev. Lett. 35 1124(1975).
16. P.B. Wilson et al., SLAC report number SLAC-PUB-1894 (1977).
17. In our error analysis, we have assigned the error due to the long-term drift in  $E_b$  determination to be 0.5 MeV. This is probably conservative.

18. G. Goldhaber *et al.*, Phys. Rev. Lett. 37, 255(1976); I. Peruzzi *et al.*, Phys. Rev. Lett. 37, 569(1976).
19. V. Lüth *et al.*, SLAC report number SLAC-PUB-1947 (1977).
20. D.B. Lichtenberg, Phys. Rev. D 12, 3760(1975); A. De Rújula, H. Georgi, and S.L. Glashow, Phys. Rev. Lett. 37, 398(1976); K. Lane and S. Weinberg, Phys. Rev. Lett. 37 717(1976); S. Ono, Phys. Rev. Lett. 37, 655(1976); W. Celmaster, Phys. Rev. Lett. 37, 1042(1976); H. Fritzsch, Phys. Lett. 63B, 419(1976); J. Dabaul and M. Krammer, Phys. Lett. 64B, 341(1976); N.G. Deshpande *et al.*, Phys. Rev. Lett. 37, 1305(1976); J.S. Guillen, Lett. al Nuovo Cimento 18, 218(1977); D.H. Boal and A.C.D. Wright, University of Alberta report (1976); L.H. Chan, Louisiana State University report (1976); D.C. Peaslee, Phys. Rev. D15, 3495(1977); and N.F. Nasrallah and K. Schilcher, Universität Mainz report NZ-TH 76/15 (1976).
21. The value is from the "normal fit" of Ref. 4. The "isospin constrained fit" gave an erroneous value for  $B(D^{0*} \rightarrow D^0\gamma)$  because the  $D^+$  mass was fit to be 1873 MeV/c<sup>2</sup>. This forbade the decay  $D^{*+} \rightarrow D^+\pi^0$  and forced all  $D^{*+} \rightarrow D^+$  decays into the mode  $D^{*+} \rightarrow D^+\gamma$ , which in turn forced too high a value of  $B(D^{0*} \rightarrow D^0\gamma)$  through the constraint conditions.
22. See F.J. Gilman in these proceedings for a discussion of the validity of these models for ordinary quarks.
23. G. Altarelli, N. Cabibbo, L. Maiani, Nucl. Phys. B88, 285(1975); R.L. Kingsley, S.B. Treiman, F. Wilczek, and A. Zee, Phys. Rev. D11, 1919(1975); M.B. Einhorn and C. Quigg, Phys. Rev. D12, 2015(1975).
24. J.L. Rosner, Invited talk at Orbis Scientiae, Jan. 17-21, 1977, Coral Gables, Fla., (Institute for Advanced Study report COO-2220-120).
25. See W. De Boer in these proceedings for a discussion of the evidence for F production at 4.4 GeV.
26. A. De Rújula, H. Georgi, and S.L. Glashow, Phys. Rev. Lett. 317(1977). M. Bander, University of California at Irvine report UCI 77-32 (1977).
27. A. Pais and S.B. Treiman, Phys. Rev. D15, 2529(1977).
28. See V. Lüth in these proceedings for a discussion of how this is done for total charged multiplicities.
29. See M.L. Perl in these proceedings.